

# Reproducing the assembly of massive galaxies within the hierarchical cosmogony

Fabio Fontanot<sup>1,2</sup>, Pierluigi Monaco<sup>2,3</sup>, Laura Silva<sup>3</sup>, Andrea Grazian<sup>4</sup>

<sup>1</sup>Max-Planck-Institute for Astronomy, Königstuhl 17, D-69117, Heidelberg, Germany

<sup>2</sup>Dipartimento di Astronomia, Università di Trieste, via Tiepolo 11, 34131 Trieste, Italy

<sup>3</sup>INAF-Osservatorio Astronomico di Trieste, via Tiepolo 11, 34131 Trieste, Italy

<sup>4</sup>INAF-Osservatorio Astronomico di Roma, via Frascati 33, I-00040Monteporzio, Italy

email: fontanot@mpia-hd.mpg.de; monaco, silva@oats.inaf.it; grazian@mporzio.astro.it

Accepted ... Received ...

## ABSTRACT

In order to gain insight into the physical mechanisms leading to the formation of stars and their assembly in galaxies, we compare the predictions of the MOdel for the Rise of GALaxies aNd Active nuclei (MORGANA) to the properties of  $K$ - and  $850\mu$ -selected galaxies (such as number counts, redshift distributions and luminosity functions) by combining MORGANA with the spectrophotometric model GRASIL. We find that it is possible to reproduce the  $K$ - and  $850\mu$ -band datasets at the same time and with a standard Salpeter IMF, and ascribe this success to our improved modeling of cooling in DM halos. We then predict that massively star-forming discs are common at  $z \sim 2$  and dominate the star-formation rate, but most of them merge with other galaxies within  $\sim 100$  Myr. Our preferred model produces an overabundance of bright galaxies at  $z < 1$ ; this overabundance might be connected to the build-up of the diffuse stellar component in galaxy clusters, as suggested by Monaco et al. (2006), but a naive implementation of the mechanism suggested in that paper does not produce a sufficient slow-down of the evolution of these objects. Moreover, our model over-predicts the number of  $10^{10} - 10^{11} M_{\odot}$  galaxies at  $z \sim 1$ ; this is a common behavior of theoretical models as shown by Fontana et al. (2006). These findings show that, while the overall build-up of the stellar mass is correctly reproduced by galaxy formation models, the “downsizing” trend of galaxies is not fully reproduced yet. This hints to some missing feedback mechanism in order to reproduce at the same time the formation of both the massive and the small galaxies.

**Key words:** galaxies: formation – galaxies: evolution

## 1 INTRODUCTION

The Lambda Cold Dark Matter ( $\Lambda$ CDM) cosmology is consistent with a large body of observations of the large-scale Universe (see, e.g., Spergel et al. 2006). Then, the predicted hierarchical evolution of Dark Matter (DM) perturbations subject to gravitational instability provides a standard framework to study the formation and evolution of luminous structures in the Universe. However, while the cosmological framework is fixed with a small uncertainty, several open questions, regarding to the formation and evolution of galaxies, arise from the complex evolution of baryons within the potential wells of the DM halos.

Galaxy formation is observationally constrained by many multi wavelength surveys of deep fields (e.g. COMBO17, Wolf et al., 2001; DEEP2, Davis et al., 2003; GOODS, Giavalisco et al. 2004; GEMS, Rix et al. 2004; UKIDSS, Lawrence et al., 2006; COSMOS, Scoville et al.,

2007; etc.). To compare with these datasets, many thousands of galaxies must be generated by models. This makes a straightforward numerical approach problematic (it has been attempted, e.g. by Nagamine et al. 2005, Saro et al., 2006, Robertson et al. 2007), so that simpler and quicker models have been developed, based on sets of recipes that address the various processes involved. These “semi-analytical” models (see e.g. Somerville et al. 2001, 2004; Granato et al. 2004; Menci et al., 2004; Baugh et al. 2005; Kang et al., 2005; Bower et al., 2006; Croton et al. 2006; Cattaneo et al., 2006; De Lucia et al., 2006; Monaco, Fontanot & Taffoni, 2007) have been tested against an impressive number of observational constraints. In this decade-long testing process, many specific models have been unsuccessful in reproducing constraints like the high-mass cutoff of the luminosity function (Benson et al. 2003), the level of  $\alpha$ -enhancement in elliptical galaxies (Thomas 2005; Na-

gashima et al., 2005), the redshift distribution of K-band sources (Cimatti et al. 2002a), the surface density of EROs (Cimatti et al. 2002b, Daddi et al. 2002; Smith et al. 2001).

Many of these difficulties have been overcome by later versions of the models, but some of them have required strong assumptions: for instance, a top-heavy IMF in starbursts is required by Baugh et al. (2005) to reproduce the sub-mm counts. In the most recent models (see i.e. Bower et al. 2006; Croton et al., 2006) the cutoff of the galaxy luminosity function and the bimodality of galactic colors is obtained only if cooling flows in large halos are quenched by AGN feedback, i.e. by the energy emerging from massive black holes accreting at a relatively low rate (in the so-called *radio mode*).

A recently highlighted observational trend of galaxy formation is the so-called *downsizing* of galaxies: at variance with the hierarchical trend of DM halos, more massive galaxies tend to form their stars earlier and in a shorter period than smaller galaxies, which experience more prolonged star-formation histories. While this general trend is known to be not incompatible with cosmology once stellar and AGN feedback are properly taken into account (see, e.g., Granato et al., 2004; Neisteinn, van den Bosch & Dekel, 2006), recent observations show that the details, like for instance the (almost) parallel evolution of the star formation density for galaxies of different mass (Zheng et al. 2007), are still not reproduced.

Massive elliptical galaxies have always been remarkably elusive objects in this regard. The first versions of hierarchical galaxy formation models (see, e.g. White 1996) predicted that these galaxies form late ( $z \sim 1$ ) by the merging of already assembled discs, while evidence from stellar populations (see Matteucci 1996 for a review), the tightness of the fundamental plane (Renzini & Ciotti, 1993), the evolution of the color-magnitude relation (Kodama et al., 1998; Blakeslee et al., 2003; Ellis et al. 2006) and the local  $M_{g2} - \sigma$  relation (Bernardi et al. 2003) suggested that they formed early ( $z > 2$ ) in a short burst of star formation. Clearly, in a hierarchical Universe the age of stars does not need to coincide with the assembly age of the galaxy, defined as the time at which the most massive progenitor has at least half of the final stellar mass. Massive ellipticals could then be assembled late by *dry mergers* of other ellipticals, so as to preserve the oldness of their stellar populations while producing a low assembly redshift (De Lucia et al. 2006). This possibility is severely constrained by the modest (if any) evolution of the high end of the stellar mass function since  $z = 1$  (Cimatti, Daddi & Renzini, 2006): while models predict a doubling of stellar masses (De Lucia & Blaizot, 2007), evidence excludes an evolution larger than  $\sim 0.2$  dex (as roughly estimated by Monaco et al. 2006; see the references therein). Recently, Monaco et al. (2006; see also Conroy, Weschler, & Kravtsov, 2007) have proposed that the formation of a diffuse stellar component in galaxy clusters by scattering of stars during dry mergers (see, e.g., Murante et al. 2007) may conspire to decrease the expected evolution of the high end of the stellar mass function.

The early formation of massive galaxies and their following (almost passive) evolution are best constrained by deep observations in the sub-mm band, suited to reveal obscured star formation events at high redshift, and in the K-band, suited to probe stellar masses at lower redshift.

The warm dust present in star forming clouds absorbs most of the UV/blue photons emitted by young stars and re-processes them to the FIR, becoming the dominant contributor in that band. Moreover, the steeply decreasing shape of the galactic SEDs from  $\sim 100\mu\text{m}$  to  $\sim 1$  mm gives a negative K-correction that promotes the observation of starbursts in the sub-mm bands up to  $z \sim 5$ . Therefore strong starbursts at high redshift are more easily observed in the sub-mm than in the optical. The sub-mm emission is measurable in a few windows, most notably that at  $850\mu\text{m}$ . Observations with the Submillimeter Common-User Bolometer Array (SCUBA) on the James Clerk Maxwell Telescope have highlighted the presence of a population of high-redshift massive starbursts (see, e.g., Smail et al. 1997; Hughes et al. 1998; Chapman et al. 2002; Scott et al. 2002) commonly interpreted as galaxies forming stars at rates of hundreds if not thousands of  $M_{\odot} \text{ yr}^{-1}$ . Given the poor angular resolution of SCUBA images, the identification of optical counterparts is difficult, and can be achieved using interferometric images at longer wavelengths. The resulting redshift distribution is thought to peak at  $z \sim 2.4$  (Chapman et al. 2003, 2005).

The K-band is a very good tracer of the stellar mass at  $z \lesssim 1.5$  (Gavazzi et al. 1996), it is almost unaffected by dust extinction, and requires small K-corrections that weakly depend on the morphological type, so it is ideal to follow the assembly of the bulk of stellar mass. The local K-band LF has been measured with great accuracy by the 2MASS collaboration (Cole et al. 2001; Kochanek et al. 2001). In this paper we will focus on four K-band surveys with (photometric or spectroscopic) redshift coverage. (i) The K20 survey (Cimatti et al. 2002a, Pozzetti et al. 2003) is a  $K < 20$  (corresponding to  $K_{AB} < 21.84$ ) limited sample, covering  $52\text{arcmin}^2$ , with a very high redshift completeness ( $> 90\%$ ). (ii) The GOODS-MUSIC (Grazian et al. 2006) catalogue is a multi-color sample extracted from the deep and wide survey conducted over the Chandra Deep Field South in the framework of the GOODS project. Here we use the  $K_{AB} < 23.5$  limited galaxy sample defined in Fontana et al. (2006). This sample covers  $143.2\text{arcmin}^2$ ; 28% of the galaxies have a spectroscopic redshifts, used to train photometric redshift estimates for all other galaxies. (iii) The UKIDSS Ultra Deep Survey (UDS, Dye et al., 2006) galaxy sample is a complete catalog of  $K_{AB} < 22.5$  selected galaxies over  $0.6\text{deg}^2$ ; for each object in the sample a photometric estimate of the redshift is provided. (iv) The VIMOS-VLT Deep Survey (VVDS) (Le Fevre et al., 2005) is a spectroscopic survey designed to measure redshift for  $\sim 10^5$  sources selected, nearly randomly from a photometric catalogue. Here we consider a K-selected sample, with either photometric and spectroscopic redshifts obtained by Pozzetti et al. (2007) combining a  $K_{AB} < 22.34$  limited sample (20% redshift completeness) defined over a  $442\text{arcmin}^2$  area, with a  $K_{AB} < 22.84$  limited sample (29% redshift completeness) defined over a  $172\text{arcmin}^2$  area.

This paper is the third of a series devoted to describe the MOdel for the Rise of GALaxies aNd Active nuclei (MORGANA). With respect to similar models of galaxy formation, MORGANA presents a different, more sophisticated treatment of the mass and energy flows between galactic phases (cold and hot gas, stars) and components (bulge, disc, halo). In particular, the process of radiative cooling of the shocked gas is treated with a new model (tested against simulations

in Viola et al., in preparation), while feedback is inserted following the model by Monaco (2004) and galaxy winds and super-winds are allowed. The model is described in detail in Monaco, Fontanot & Taffoni (2007; hereafter paper I). The prediction of the properties of the AGN population is presented in Fontanot et al. (2006; hereafter paper II), and the prediction of the evolution of the stellar mass function, together with those of other similar models, has been compared to the results inferred from the GOODS-MUSIC data in Fontana et al. (2006). As mentioned above, MORGANA has been used by Monaco et al. (2006) to address the lack of evolution of the high end of the stellar mass function and its connection with the building of the diffuse stellar component in galaxy clusters. In this paper we compare the predictions of MORGANA to the data mentioned above of deep fields in sub-mm (850  $\mu\text{m}$ ) and  $K$  bands to test to what extent the model is able to reproduce the formation and assembly of massive galaxies. To this aim, we have combined MORGANA with the spectrophotometric code GRASIL (Silva et al. 1998) that computes the UV to radio SEDs of model galaxies, including a three-dimensional bulge+disk geometry with a two-phase interstellar medium, the radiative transfer through the dusty ISM, a realistic dust grain model, and a direct computation of the dust temperature distribution.

The paper is organized as follows. In section 2.1 we describe the main properties of the MORGANA model. In section 2.2 we describe how we compute luminosity functions, number counts and redshift distributions interfacing the output of the model with GRASIL. In section 3 we present our results, a discussion is given in Section 4, and in Section 5 we give our conclusions. Throughout this work we assume, whenever necessary, the concordance cosmological model  $\Omega_\Lambda = 0.7$ ,  $\Omega_m = 0.3$ ,  $H_0 = 70 \text{ K m s}^{-1} \text{ Mpc}^{-1}$ ,  $\sigma_8 = 0.9$ .

## 2 MODEL

### 2.1 Galaxy formation model: MORGANA

MORGANA is described in full detail in Monaco, Fontanot & Taffoni (2007), while AGN accretion is described in Fontanot et al. (2006). We give here only a brief description, aimed at highlighting the main processes included in the model.

#### 2.1.1 Algorithm

MORGANA follows the typical scheme of semi-analytic models, with some important differences. Each DM halo contains one galaxy for each progenitor<sup>1</sup>; the galaxy associated with the main progenitor is the central galaxy. Baryons in a DM halo are divided into three components, namely a halo, a bulge and a disc. Each component contains three phases, namely cold gas, hot gas and stars. For each component the

code follows the evolution of its mass, metal content, thermal energy of the hot phase and kinetic energy of the cold phase.

The main processes included in the model are the following.

(i) The merger trees of DM halos are obtained using the PINOCCHIO tool (Monaco et al. 2002; Monaco, Theuns & Taffoni 2002; Taffoni, Monaco & Theuns 2002).

(ii) After a merging of DM halos, dynamical friction, tidal stripping and tidal shocks on the satellite (the smaller DM halo, with its galaxy at the core) lead to a merger with the central galaxy or to tidal destruction as described by Taffoni et al. (2003). At each merger a fraction of the satellite stars is scattered to the stellar halo component (Murante et al. 2007; Monaco et al. 2006). These stars are not associated to galaxies but to the intra-cluster light.

(iii) The evolution of the baryonic components is performed by numerically integrating a system of equations for all the mass, energy and metal flows; this allows not to be restricted to linear dynamics.

(iv) The intergalactic medium infalling on a DM halo is shock-heated, as well as the hot halo component of merging satellites (which is given to the main halo) and that of the main halo in case of major merger ( $M_{\text{sat}} > 0.2 \times M_{\text{tot}}$ ). Following Wu, Fabian & Nulsen (2001), shock-heating is implemented by assigning to the infalling gas a specific thermal energy equal to 1.2 times the specific virial energy,  $-0.5 U_{\text{H}}/M_{\text{H}}$  (where  $M_{\text{H}}$  and  $U_{\text{H}}$  are the mass and binding energy of the DM halo).

(v) The profile of the hot halo gas is computed at each time-step by solving the equation for hydrostatic equilibrium with a polytropic equation of state and an assumed polytropic index  $\gamma_p = 1.2$ . No hot gas is present within a cooling radius  $r_{\text{cool}}$ , which is set to a vanishingly small value at major mergers.

(vi) The cooling flow is computed by integrating the contribution to radiative cooling of each spherical shell, taking into account the heating from (stellar and AGN) feedback from galaxies. Given the importance of cooling for the results presented in this paper, we give here some detail of the cooling model. If  $T_{g0}$  and  $\rho_{g0}$  are the temperature and density of the hot halo gas extrapolated to  $r = 0$ ,  $\mu_{\text{hot}} m_p$  its mean molecular weight and  $r_s = r_{\text{H}}/c_{\text{nfw}}$  the scale radius of the halo (of radius  $r_{\text{H}}$  and concentration  $c_{\text{nfw}}$ ), then the mass cooling flow  $\dot{M}_{\text{co,H}}$  results:

$$\dot{M}_{\text{co,H}} = \frac{4\pi r_s^3 \rho_{g0}}{t_{\text{cool},0}} \times \mathcal{I}(2/(\gamma_p - 1)) \quad (1)$$

where the integral  $\mathcal{I}(\alpha)$  is defined as  $\int_{r_{\text{cool}}/r_s}^{c_{\text{nfw}}/r_s} \{1 - a[1 - \ln(1 + t)/t]\}^\alpha t^2 dt$ , with  $a = [3T_{\text{vir}}(\gamma_p - 1)c_{\text{nfw}}(1 + c_{\text{nfw}})] / \{\gamma_p T_{g0}[(1 + c_{\text{nfw}}) \ln(1 + c_{\text{nfw}}) - c_{\text{nfw}}]\}$  ( $T_{\text{vir}}$  being the virial temperature of the halo). The cooling time  $t_{\text{cool},0}$  is computed using the central density (the density gradient is taken into account by the integral  $\mathcal{I}$ ) and the temperature at  $r_{\text{cool}}$  (the temperature gradient is neglected):

$$t_{\text{cool},0} = \frac{3kT_g(r_{\text{cool}})\mu_{\text{hot}}m_p}{2\rho_{g0}(\Lambda_{\text{cool}} - \Gamma_{\text{heat}})} \quad (2)$$

Here  $\Lambda_{\text{cool}}$  is the metal-dependent Sutherland & Dopita (1993) cooling function and the heating term  $\Gamma_{\text{heat}}$  is computed assuming that the energy flow  $\dot{E}_{\text{hw,H}}$  fed back by the galaxy is given to the cooling shell:

<sup>1</sup> Each DM halo forms through the merging of many halos of smaller mass, called progenitors. At each merging the largest halo survives (it retains its identity), the others become substructure of the largest one. The main progenitor is the one that survives all the mergings. The mass resolution of the box used for computing the merger trees sets the smallest progenitor mass, as explained in section 2.1.2.

$$\Gamma_{\text{heat}} = \frac{\dot{E}_{\text{hw,H}}}{4\pi r_s^3 \mathcal{I}(2/(\gamma_p - 1))} \left( \frac{\mu_{\text{hot}} m_p}{\rho_{g0}} \right)^2 \quad (3)$$

Whenever  $\Gamma_{\text{heat}} > \Lambda_{\text{cool}}$  the cooling flow is quenched. The cooling radius  $r_{\text{cool}}$  is treated as a dynamical variable whose evolution takes into account the hot gas injected by the central galaxy ( $\dot{M}_{\text{hw,H}}$ ):

$$\dot{r}_{\text{cool}} = \frac{\dot{M}_{\text{co,H}} - \dot{M}_{\text{hw,H}}}{4\pi \rho_g(r_{\text{cool}}) r_{\text{cool}}^2}. \quad (4)$$

This equation is valid if pressure is balanced at  $r_{\text{cool}}$ , an assumption which clearly does not hold in general. We mimic the pressure force acting on mass shell at  $r_{\text{cool}}$  as follows:

$$\dot{r}'_{\text{cool}} = \dot{r}_{\text{cool}} - c_s \quad (5)$$

where  $c_s$  is the sound speed computed at  $r_{\text{cool}}$ . This recipe is different from that used in most other semi-analytical models, where a cooling radius is computed by inverting the cooling time as a function of radius. Viola et al. (2007) have compared analytic cooling models to N-body + hydro simulations showing that, while the "classical" cooling model significantly underestimates the amount of cooled mass, the present cooling model gives a very good fit.

(vii) When the hot halo phase is heated by feedback beyond the virial temperature, it can leave the DM halo in a galactic super-wind. A similar thing happens to the cold halo gas when it is accelerated by stellar feedback. To compute the time at which the ejected gas falls back into a DM halo, its merger history is scrolled forward in time until the circular velocity is larger than the (sound or kinetic) velocity of the gas at the ejection time.

(viii) The cooling gas is let infall on the central galaxy on a dynamical time-scale (computed at  $r_{\text{cool}}$ ). It is divided between disc and bulge according to the fraction of the disc that lies within the half-mass radius of the bulge.

(ix) The gas infalling on the disc keeps its angular momentum; disc sizes are computed with an extension of the Mo, Mao & White (1998) model that includes the contribution of the bulge to the disc rotation curve.

(x) Disc instabilities and major mergers of galaxies lead to the formation of bulges. We also take into account a possible disc instability driven by feedback. In minor mergers the satellite mass is given to the bulge component of the larger galaxy.

(xi) Star formation and feedback in bulges and discs are inserted following the model of Monaco (2004). According to that model, the regime of stellar feedback in a galaxy depends mainly on the density and vertical scale-length of the galactic system. In thin systems, like spiral discs with gas surface density  $\Sigma_{\text{cold,D}}$  and fraction of cold gas  $f_{\text{cold,D}}$ , the timescale for star formation  $t_{\star,\text{D}}$  is predicted to be:

$$t_{\star,\text{D}} = 9.1 \left( \frac{\Sigma_{\text{cold,D}}}{1 \text{ M}_{\odot} \text{ pc}^{-2}} \right)^{-0.73} \left( \frac{f_{\text{cold,D}}}{0.1} \right)^{0.45} \text{ Gyr} \quad (6)$$

Due to the correlation of  $f_{\text{cold,D}}$  and  $\Sigma_{\text{cold,D}}$  (galaxies with higher gas surface density consume more gas), this relation is compatible with the Schmidt law. Thick systems like star-forming bulges (or mergers) are dominated by transients which are very difficult to model, so the straightforward Schmidt law is used:

$$t_{\star,\text{B}} = 4 \left( \frac{\Sigma_{\text{cold,B}}}{1 \text{ M}_{\odot} \text{ pc}^{-2}} \right)^{-0.4} \text{ Gyr} \quad (7)$$

In both cases, hot gas is ejected to the halo (in a hot galactic wind) at a rate equal to the star-formation rate (as predicted by Monaco 2004), though massive bulges with circular velocity  $V_B \gtrsim 300 \text{ km s}^{-1}$  are able to bind their hot phase component. The thermal energy of this re-heated gas is not scaled to the DM halo circular velocity but to the energy of exploding SNe.

(xii) In star-forming bulges cold gas is ejected in a cold galactic wind by kinetic feedback due to the predicted high level of turbulence driven by SNe (this process is described in full detail in paper II, Section 2.2).

(xiii) Accretion of gas onto massive black holes (starting from small seeds present in all galaxies) is connected to the ability of cold gas to loose angular momentum by some (unspecified) mechanism driven by star formation. This is explained in full detail in paper II.

(xiv) Because accretion onto black holes is triggered by star formation, AGN feedback can quench cooling flows only after their start. Alternatively, the cooling flow can be quenched when a fiducial energy criterion is met, without letting any gas fall to the galaxy and form stars. This "forced quenching" procedure has been used in paper II and will be discussed in a forthcoming paper.

(xv) Metal enrichment is self-consistently modeled in the instantaneous recycling approximation.

### 2.1.2 Runs

All models are based on the same PINOCCHIO run we introduced in paper I, a 512<sup>3</sup> realization of a 150Mpc comoving box ( $h = 0.7$ ). The mass particles is  $1.0 \times 10^9 \text{ M}_{\odot}$ , and the smallest halo we consider contains 50 particles, for a mass of  $5.1 \times 10^{10} \text{ M}_{\odot}$ . The branches of the DM halo merger trees are tracked starting from a mass of 10 particles, corresponding to  $1.0 \times 10^{10} \text{ M}_{\odot}$ ; this is the mass of the smallest progenitors. For sake of comparison, the corresponding values for the Millennium Simulation (Springel et al. 2005) are  $1.2 \times 10^9$  for the particle mass and  $2.5 \times 10^{10}$  for the smallest progenitor. We have tested the overall stability of our results by running the model over two other 512<sup>3</sup> boxes of size 200 and 100 Mpc (see paper I for more details).

The stellar mass of the typical galaxy contained in the smallest DM halo at  $z = 0$  is  $3 \times 10^8 \text{ M}_{\odot}$ . In order to estimate the completeness limit for the stellar mass function we consider an higher resolution PINOCCHIO run (512<sup>3</sup> realization of a 100Mpc comoving box, see also paper I, appendix B, for a discussion about the numerical stability of the model). We study the typical stellar mass of the galaxies belonging to  $2.5 - 5.1 \times 10^{10} \text{ M}_{\odot}$  DM halos and we estimate a completeness limit of  $4.5 \times 10^8 \text{ M}_{\odot}$ . For each run we compute the evolution of (up to) 300 trees (i.e. DM halos at  $z = 0$ ) per logarithmic bin of halo mass of width 0.5 dex. This implies that while all the most massive halos are considered, smaller halos are randomly sparse-sampled. To properly reconstruct the statistical properties of galaxies we assign to each tree a weight  $w_{\text{tree}}$  equal to the inverse of the fraction of selected DM halos in the mass bin.

A standard parameter choice was presented in paper I. However, it was noticed there that spiral discs tend to be more compact than in the real Universe. A Schmidt-Kennicutt-like law (equation 6) is used to compute star formation rates, so this results in higher surface densities,

shorter star formation timescales and lower gas fractions at  $z = 0$ . Forcing DM halo concentrations to lower values allows to alleviate this problem, while reproducing the zero-point of the Tully-Fisher relation and preserving a good fit of the Schmidt-Kennicutt law. We then scale concentrations so as to take a given value for a  $10^{12} M_{\odot}$  DM halo at  $z = 0$ . The value was proposed to be 4 in paper I; however, we noticed that this choice tends to lower the stellar mass function at the knee, so we use the slightly higher value of 6 as a good compromise. Moreover, following Monaco et al. (2006) we scatter to the halo stellar component 40% of the stellar mass of satellites at each galaxy merger. Finally, we implement AGN feedback by adopting the “forced quenching” procedure of paper II; this choice has little influence on the results presented here, and will be discussed in a forthcoming paper. Also, we have checked that the inclusion of quasar-triggered galaxy winds, necessary to reproduce the accretion history of massive black holes (paper II), does not change the qualitative behavior of the models.

These changes of parameters do not influence in any way the conclusions drawn in this paper. In fact, we are not proposing a “best fit” model of the galaxy population; on the contrary, we will show that MORGANA is able to reproduce many observables, but its agreement with data breaks as soon as one tries to reproduce some relevant aspects of the “downsizing” trend, so that a global fine-tuning of the model is not possible. The most important point of such an investigation is to understand the limits of these models and the origin of the disagreement with data. Fine-tuning to fit specific datasets, like the local luminosity functions, will be required in other contexts, for instance to create galaxy mock catalogues.

## 2.2 SED model: GRASIL

For each galaxy modeled by MORGANA we compute the corresponding UV to radio SED with GRASIL. The details of the code are given in Silva et al. (1998) (and the subsequent updates and improvements in Silva 1999; Granato et al. 2000; Bressan, Silva, Granato 2002; Panuzzo et al. 2003; Vega et al. 2005), while we summarize here the main features. (i) Stars and dust are distributed in a bulge (King profile) + disk (radial and vertical exponential profiles) axisymmetric geometry. (ii) We consider the clumping of both (young) stars and dust, through a two-phase interstellar medium with dense giant molecular clouds (MCs) embedded in a diffuse (“cirrus”) phase. (iii) The stars are assumed to be born within the optically thick MCs and gradually to escape from them as they get older on a time-scale  $t_{\text{esc}}$ . This gives rise to an age-selective extinction, with the youngest and most luminous stars suffering larger dust extinction than older ones. (iv) The dust consists of graphite and silicate grains with a distribution of grain sizes, and Polycyclic Aromatic Hydrocarbons (PAH) molecules. In each point of the galaxy and for each grain type the appropriate temperature is computed (either equilibrium  $T$  for big grains or probability distribution of temperature for small grains and PAHs). The detailed PAH emission spectrum has been updated in Vega et al. (2005) based on the Li & Draine (2001) model. (v) The radiative transfer of starlight through the dust distribution is computed yielding the emerging SED. The simple stellar population (SSP) library (Bressan, Granato, & Silva 1998;

**Table 1.** Adopted values for the GRASIL parameters that are not provided by MORGANA.

Parameters	Values
$t_{\text{esc}}$	$10^7$ yr
$f_{\text{MC}}$	0.5
$M_{\text{MC}}/r_{\text{MC}}^2$	$10^6 M_{\odot}/(16 \text{ pc})^2$
$h_d^*/r_d^*$	0.1
$h_d^d/r_d^d$	0.1

Bressan et al. 2002) includes the effect of the dusty envelopes around AGB stars, and the radio emission from synchrotron radiation and from ionized gas in HII regions.

The GRASIL parameters that are not provided by MORGANA are summarized in Table 1, and are described in the following. (i) The escape time-scale of young stars for the parent MCs is set to  $t_{\text{esc}} = 10^7$  yr. This is intermediate between the values found by Silva et al. (1998) to well describe the SED of spirals ( $\sim$  a few Myr) and starbursts ( $\sim$  a few 10 Myr), and is of the order of the estimated destruction time scale of MCs by massive stars (e.g. Monaco et al 2004b). (ii) The gas mass predicted by MORGANA is subdivided between the dense and diffuse phases, fixing the fraction of gas in molecular clouds  $f_{\text{MC}}$  to 0.5. The resulting SEDs are not much sensitive to this choice. (iii) The mass of dust is obtained by the gas mass and the dust to gas mass ratio  $\delta$  which is set to evolve linearly with the metallicity ( $\delta = 0.45 Z$ ). (iv) The optical depth of MCs, driving their spectrum, depends on the mass and radius set for MCs through  $\tau \propto \delta M_{\text{MC}}/r_{\text{MC}}^2$ , with  $M_{\text{MC}} = 10^6 M_{\odot}$ ,  $r_{\text{MC}} = 16$  pc; (iv) the bulge and disk scale radii for stars and gas are given by MORGANA, while the disk scale heights,  $h_d^*$  and  $h_d^d$  for stars and dust respectively, are set to 0.1 the corresponding scale radii. In addition, the dust grain size distribution and abundances are set to match the mean Galactic extinction curve and emissivity (as in Silva et al. 1998 and Vega et al. 2005) and are not varied here.

## 2.3 Interfacing MORGANA with GRASIL

The output of MORGANA consists, for each galaxy, in a time sampling of the main dynamical variables of the model: for each component (halo, bulge, disc) the code issues mass, kinetic energy and metal mass of cold gas; mass, thermal energy and metal mass of hot gas; mass and metals of stars; average (over the time bin) and punctual (at the end of the time bin) star formation rate (these are given only for bulge and disc). For each galaxy it gives also expelled mass and metals, black hole mass, cooling radius, bulge and disc radii and velocities, punctual values of the accretion rate onto the black hole. Star formation histories are reconstructed following all the exchanges of stellar matter between galaxies and galaxy components, so that they refer to the stars contained in the component at a given time and not to the stars formed in that component.

Of this information GRASIL uses the star formation and cold gas metallicity history for bulge and disk, the mass of gas in the two components at the required galactic age, and the stars and gas scale radii at the same age. The time sam-

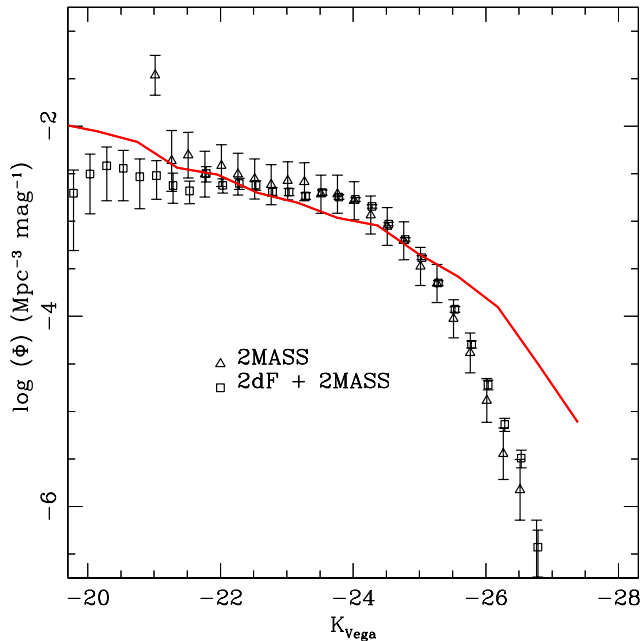


**Figure 1.** *K*-band Luminosity Function. Data refer to the observations of Cole et al. (2001) and Kochanek et al. (2001). Solid line refers to MORGANA prediction.

pling of these quantities is 0.1 Gyr. GRASIL resamples the star formation histories on a much finer time grid to optimally account for the short lifetimes of massive stars. However, the width of the time bin of MORGANA is rather large, so the number of massive stars can be rather inaccurate. We then split the last time bin into a sub-bin of 10 Myr, to which we assign the punctual value of the star-formation rate at the end of the bin, and a larger, earlier one of 90 Myr<sup>2</sup>, to which we assign a star formation rate such that the integral in the two sub-bins gives the correct final amount of stars. Using test star-formation histories, we have verified that this sampling allows to reproduce the magnitudes to within <0.1 mag; indeed, even the strongest star-formation events do not have associated time-scales much smaller than the time bin.

It is worth mentioning that running the spectrophotometric code on model galaxies is the main bottleneck of the computation; it is then necessary to devise strategies to optimize the computations by estimating the minimal number of galaxies needed to have a reliable result.

## 2.4 Luminosity functions, number counts and redshift distributions

To simulate a deep field, the computation of galaxy SEDs is performed on the box at several output times. As explained in paper I, the sparse-sampling of trees (section 2.1.2) results in an over-sampling of small satellites with respect to

<sup>2</sup> As the age of Universe in the assumed cosmology is 13.47 Gyrs, the time bin corresponding to  $z = 0$  is smaller than 0.1 Gyr; in this case we make the earlier bin consistently smaller than 90 Myr.

central galaxies of similar stellar mass. We correct for this over-sampling by further sparse-sampling the satellites as follows. First, we construct from the results of the run at  $z = 0$  an average curve of mass of the central galaxy as a function of DM halo mass; second, we randomly sparse-sample the satellites with a probability equal to the ratio between the weights  $w_{\text{tree}}$  of the tree the satellite belongs to and that of the DM halo whose central galaxy has on average the same mass as the satellite. The inverse of this probability is a new weight,  $w_{\text{sat}}$ . Central galaxies are all selected and assigned a unity weight. If a galaxy is destroyed by mergers (or tides) then its stellar mass at the destruction time is used to compute  $w_{\text{sat}}$ . This procedure gives a roughly constant number of galaxies in logarithmic intervals of mass. Because each galaxy is present in many time bins, the number of selected galaxies is typically very high. To limit this number we introduce a third weight  $w_{\text{gal}}$  as the inverse of a further sampling factor, equal for all galaxies. The first two samplings (of merger trees and galaxies) are both computed at  $z = 0$ , but the weights  $w_{\text{tree}}$  and  $w_{\text{sat}}$  assigned to the galaxies are used at any redshift. This is done with no loss of generality, as a fair reconstruction of luminosity functions or number counts only requires that the weights are used consistently with the sparse-sampling procedure; in other words, we only need to require that the properties of a sparsely sampled population are weighted by the inverse of the sampling probability, whatever the redshift at which the sampling is performed.

In order to ensure a smooth description of the redshift evolution of the properties of our simulated galaxies, we use the following procedure. At every integration time-bin, corresponding to a redshift  $z(t)$ , at the end of integration we apply the three sampling procedures to all the galaxies in the box and select a subsample. It is worth to notice that the random sparse sampling ensures that a different subsample of galaxies is considered at each  $z(t)$ , so that galaxies at different redshifts are not always the same galaxies seen at different times. We define a fourth weight  $w_{\text{time}}$  as the ratio between the width of the time sampling (0.1 Gyr) and the time interval span by  $l_{\text{box}}$  at  $z(t)$ . We also compute the angle subtended by a square of comoving side  $l_{\text{box}}$  at  $z(t)$ . We then compute the SEDs of model galaxies using GRASIL and we use them to estimate absolute and apparent magnitudes (both in the Vega and AB system) and infrared fluxes. We collect these informations in catalogues.

Luminosity functions, number counts, and redshift distributions of magnitude-limited samples are then computed by performing weighted sums over the galaxies using the product of the four weights defined above. Luminosity functions at high redshift are computed over the same redshift intervals as in the observations, while number counts and redshift distributions of magnitude-limited samples are computed using galaxies starting from  $z \simeq 6$ .

## 3 RESULTS

### 3.1 *K*-band

The resulting *K*-band LF at  $z = 0$  (in the Vega system) is compared in fig. 1 to that obtained using the local 2MASS sample (Jarrett et al. 2000), limited to  $K_{\text{Vega}} < 13.5$

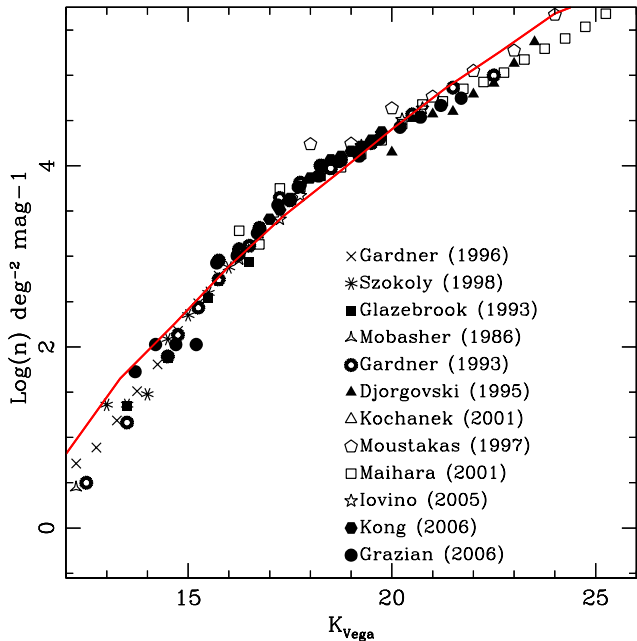


**Figure 2.** Source Number Counts in the  $K$ -band. Data refer to observations as listed in the figure. Solid line refers to MORGANA prediction.

(Kochanek et al. 2001), and the combination of the 2MASS and 2dF samples (Cole et al. 2001). Being the  $K$ -band luminosity a good tracer of stellar mass, this comparison is analogous that of figure 7 of paper I, where the stellar mass function was compared to that inferred by data (obtained also with the same 2MASS+2dF sample). In agreement with that result, the  $z = 0$   $K$ -band LF shows an overestimate of both the bright (massive) end and the faint (low-mass) end of the LF. In particular, the overestimate of the high tail is much more relevant here, with respect to the estimated mass function. We find that this is in part due to a discrepancy in the adopted  $M_*/L_K$  ratios when passing from the luminosity function to the mass function. The average  $M_*/L_K$  ratio of the MORGANA+GRASIL model galaxies is  $\sim 0.7 M_\odot/L_{K\odot}$ , while for instance Cole et al. (2001) adopt an higher average value,  $M_*/L_K = 1.32 M_\odot/L_{K\odot}$ , typical of very old stellar populations (see e.g. figure 24 in Maraston 2005). In spite of these discrepancies, the model is able to reproduce correctly the overall normalization of the LF.

Fig. 2 shows the predicted  $K$ -band number counts compared to data available in the literature (Mobasher et al. 1986; Glazebrook et al. 1993; Gardner et al. 1993, 1996; Djorgovski et al. 1995; Moustakas et al. 1997; Szokoly et al. 1998; Kochanek et al. 2001; Maihara et al. 2001; Iovino et al. 2005; Kong et al. 2006; Grazian et al. 2006). The models fit well the data in the range  $15 \lesssim K_{Vega} \lesssim 22$ . The excess at bright fluxes is a signature of the overestimate of the LF at the bright end, while the excess at faint fluxes is commented below.

Number counts do not strongly constrain the model unless redshift distributions of magnitude-limited samples are available. We then compare our results with redshift distributions obtained from the K20 (fig. 3, Vega system),

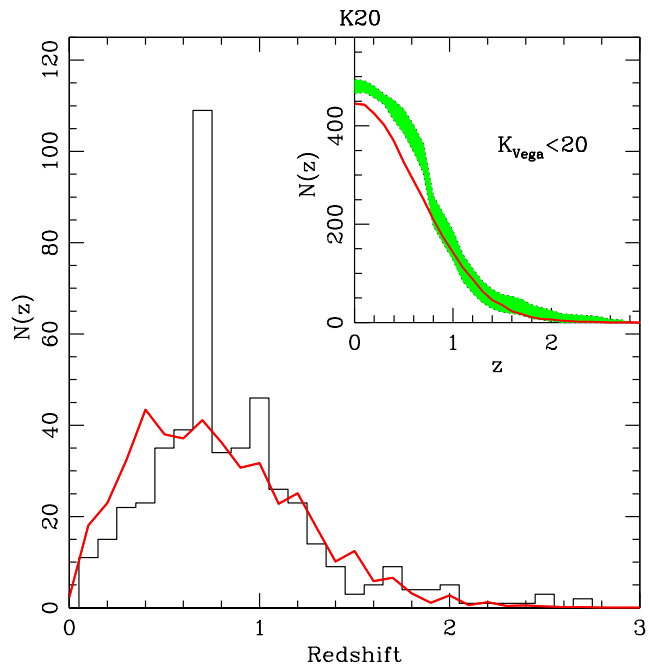


**Figure 3.** Redshift source distribution compared to K20 sample (histogram, Cimatti et al. 2002a). Solid line refers to MORGANA prediction.

GOODS-MUSIC (fig. 4, AB magnitudes) and VVDS (fig. 5, AB magnitudes) catalogues. For sake of clarity we show both the differential and the cumulative distributions. We compute the error on the cumulative distributions using a bootstrap technique based on 1000 mock redshift catalogues drawn using the observed redshift distribution. The agreement of MORGANA prediction with K20 observations (relative to  $K_{AB} < 21.84$ ) is good: we predict a total number of 435 objects against  $480 \pm 22$  observed. The position of the peak of the distribution and the long tail of galaxies at  $z > 1.5$  are both recovered; we relate the disagreement in the cumulative distribution at low redshift to the known cluster at  $z \sim 0.7$ ; some excess at  $z \sim 0.5$  can be again connected to the excess of bright galaxies in the  $K$ -band LF. The comparison with the deeper but less wide GOODS-MUSIC sample (Fig. 4) confirms the good agreement at brighter limit magnitudes (301 predicted vs 262 observed galaxies with  $K_{AB} < 20$ ; 722 predicted vs 623 observed galaxies with  $K_{AB} < 21$ ). At fainter limit magnitudes the comparison highlights an excess of model galaxies (1687 predicted vs 1258 observed galaxies with  $K_{AB} < 22$ ; 3572 predicted vs 2603 observed galaxies with  $K_{AB} < 23$ ). This excess is due not only to the small local excess noticeable in the  $z = 0$  LF (Fig. 1), but to a generalized excess of faint sources at all redshifts. Fontana et al. (2006) showed that the overprediction of small galaxies ( $M \sim 10^{10} M_\odot$ ) at  $z \sim 1$  is a common problem of galaxy formation models; here we see that the problem is probably present since high redshift. Finally, we also compare MORGANA predictions with the larger VVDS sample (Fig. 5, we combined model predictions for the two sub-samples separately in the same way as observational data): we obtain again a good agreement with observations (9822 predicted objects against 10160 observed);

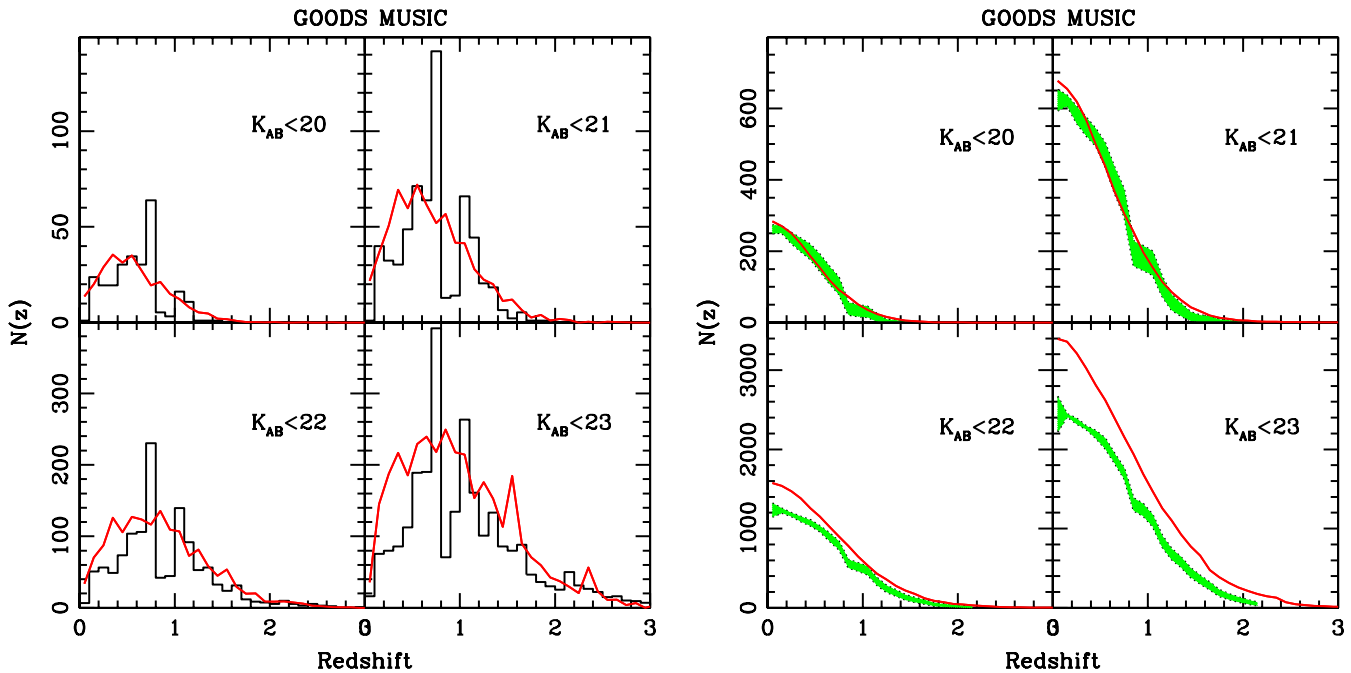


**Figure 4.** Redshift source distribution compared to GOODS-MUSIC sample (histograms, Fontana et al. 2006). Left Panel: redshift distributions. Right Panel: cumulative distributions. Solid line refers to MORGANA predictions.

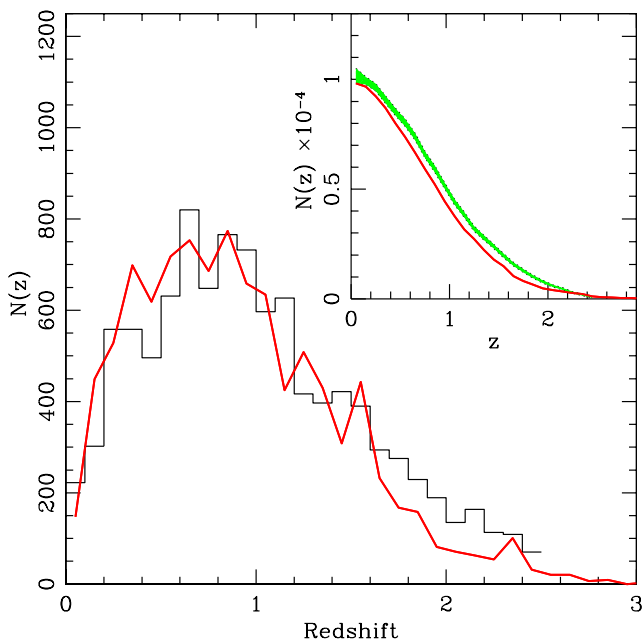


**Figure 5.** Redshift source distribution compared to VVDS sample (histogram, Pozzetti et al. 2007). Solid line refers to MORGANA prediction.

except for a mild underestimate, mostly due to the smaller number of  $z \sim 1 - 2$  objects with respect to observations.

A clearer view is obtained by considering the evolution of the K-band luminosity function with redshift (Fig. 6). We compare our model with the K20 (Pozzetti et al. 2003; Vega system) and UDS (Cirasuolo et al. 2006; AB mag-

nitudes) data; the K20 estimate is based on spectroscopic redshifts but the sampled area is small, the UDS sample covers a larger area of the sky but is based on photometric redshifts. The overall agreement between MORGANA and the two datasets is very good. We can notice some overestimate of the faint-end at  $z \sim 0.5$ , which is not as visible as in Fontana et al. (2006). Also, the lower redshift bins of the wider UDS sample show that the excess at the bright end builds up at  $z \lesssim 1$ .

From the analysis of fig. 1 to fig. 6 we conclude that MORGANA is able to reproduce the assembly of the bulk of the stellar mass, which is mostly in place already at  $z \sim 1 - 2$ ; however, the biggest model galaxies continue growing in mass at  $z < 1$ , though this growth is partially compensated for by the loss of stars to the halo by gravitational scattering. Moreover, the progressive build-up of smaller objects is not correctly reproduced; small objects tend to be too many at  $z \sim 1$  (and too old at  $z \sim 0$ ) in the model. These findings are in agreement with the analysis presented in Fontana et al. (2006).

### 3.2 850 $\mu$ m band

We now test whether the stars visible at  $z < 2$  in the K-band were formed in much smaller chunks that were later assembled together, or in big massive starbursts at  $z \gtrsim 2$ . This is best tested by comparing the model to number counts at 850 $\mu$ m, where massive starbursts at  $1 \lesssim z \lesssim 5$  are easily observed. Fig. 7 shows our prediction compared to SCUBA observations (Hughes et al. 1998; Barger et al. 1999; Eales et al. 2000; Webb et al. 2002; Borys et al. 2002, 2003; Chapman et al. 2002; Cowie et al. 2002; Scott et al. 2002; Smail et al. 2002; Coppin et al 2006; Scott et al 2006). In order to avoid contamination due to low-redshift sources, we consider



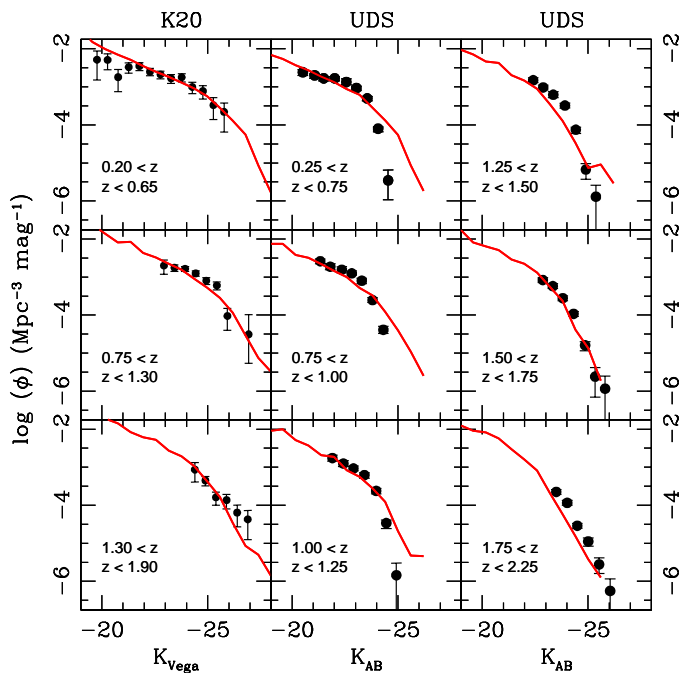


**Figure 6.** LF Redshift Evolution. Left panels: K20 sample, data points taken from Pozzetti et al. (2003). Mid and Right Panel: UDS sample, data points taken from Cirasuolo et al. (2006). Solid line refers to MORGANA predictions.

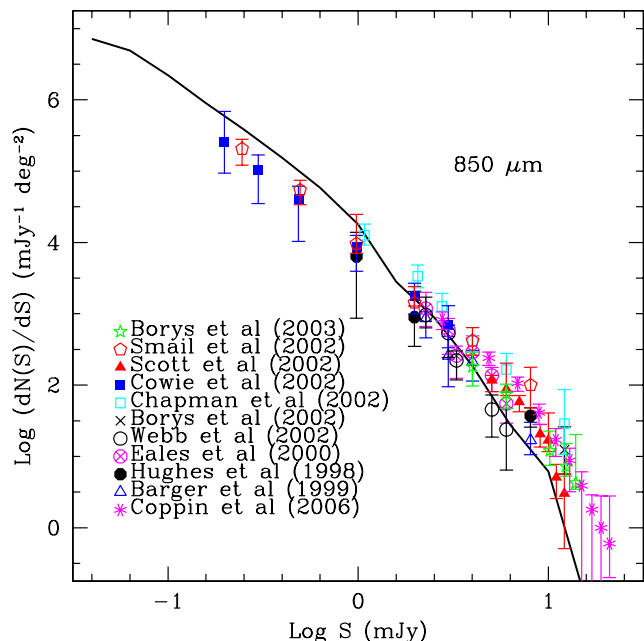


**Figure 7.**  $850\mu\text{m}$  Source Number Counts. Data refer to observations as listed in the figure. Solid line refers to MORGANA prediction.

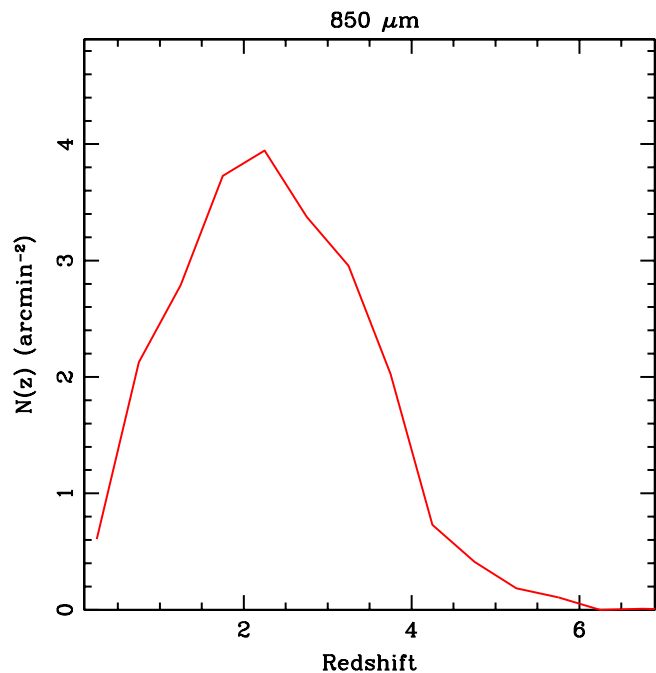


**Figure 8.** Predicted Redshift Distribution for  $850\mu\text{m}$  sources with  $S > 0.2\text{mJy}$ .

here a subsample with  $z > 0.5$ . We stress that this prediction is done assuming a standard Salpeter IMF. Fig. 8 gives the redshift distribution of the objects with flux  $> 0.2\text{mJy}$ , which corresponds to the faintest point in fig. 7. It is peaked at  $z \sim 2.0$ , in qualitative agreement with the observations of Chapman et al. (2003,2005) of the brightest SCUBA sources (redshift distribution peaked at  $z \sim 2.4$  with a quartile range of  $1.9 < z < 2.8$ ). The model reproduces well the data, with a possible modest overestimate (underestimate) at faint (bright) fluxes. However, a deeper analysis of the predictions shows that the population of brightest objects ( $> 5\text{mJy}$ ) at  $z > 2$  (Chapman et al., 2005; Aretxaga et al., 2007), is missing: we are able to reproduce the bulk of the heavily star-forming population at  $z \sim 2$ , but not the most luminous objects.

#### 4 DISCUSSION

Sub-mm counts have longly been an elusive piece of evidence to fit for semi-analytic models of galaxy formation (e.g. Guiderdoni et al. 1998; Devriendt & Guiderdoni 2000; Granato et al. 2000; but see Baugh et al. 2005). Conversely, in the long tuning and debugging process of the MORGANA code, we have never found any difficulty in fitting the bulk of number counts using a conservative choice for the IMF. The difference can be ascribed to the different cooling model that MORGANA is implementing. In a forthcoming paper (Viola et al. 2007) we compare analytic cooling models to N-body+hydro simulations in the simplest case of an isolated halo with its hot gas component initially in hydrostatic equilibrium, and no feedback from star formation or AGN. The classical model of cooling, based on the computation of a cooling radius (White & Frank 1991) is found to underestimate the amount of cooled gas, especially in the first stages

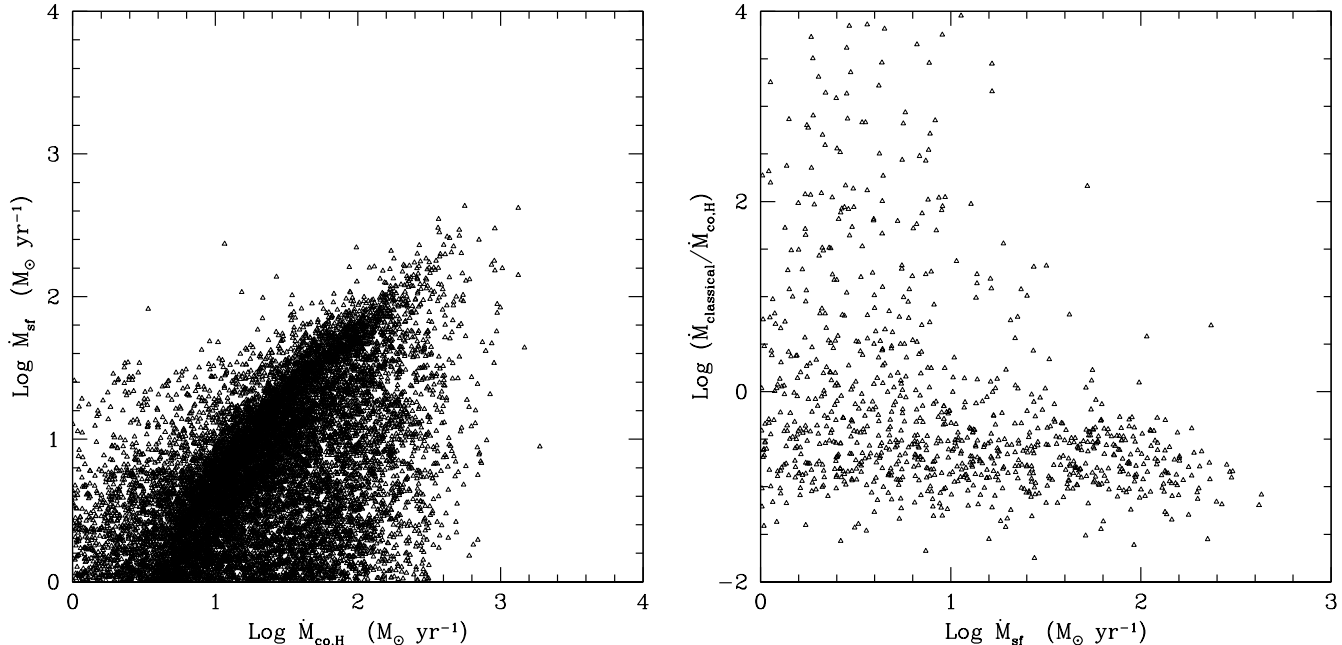


**Figure 9.** Left panel: star formation rate (bulge+disc) versus cooling rate for central galaxies at  $z = 2.5$ . Right panel: ratio of the cooling flows as predicted by the classical model and as used by MORGANA versus total star formation rate for the same galaxies as above. In the right panel many points, especially at low star-formation, lie out of the plot because the classical model predicts that all the gas has cooled, while MORGANA retains some gas through feedback and cosmological infall.

of cooling, while the model implemented in MORGANA and briefly described in Section 2.1 gives a very good fit. All the analytic models of cooling tend to give similar results at later times. The use of a better cooling model accelerates the accumulation of cold gas in the halos, giving rise to stronger starbursts. The typical mass of the halos that contain the biggest starbursts is high enough to ensure the formation of a hot halo component through shocks (see, e.g., Keres et al. 2005), so that the results based on hot gas halos in hydrostatic equilibrium apply to this case.

To support this interpretation, we run again the model, computing at each halo major merger the gas profile (as described in Section 2.1) and from it the cooling time  $t_{\text{cool}}(r)$  as a function of radius. The classical cooling radius  $r_C(t)$  is the inverse of the function  $t_{\text{cool}}(r)$ . The cooling flow of the classical cooling model is then computed as  $\dot{M}_{\text{classical}} = 4\pi r_C^2 \rho_g(r_C) dr_C/dt$ . It is not possible to use the classical cooling flow directly in the model, because the cooling model includes the injection of energy by feedback, which would then be absent. Besides, a generalization of the model to include classical cooling would require deep changes in the code and a re-calibration of the parameters to reproduce local observables, which is well beyond the interest of the paper. We then simply compare the classical cooling flow with that actually used in the MORGANA model. Firstly, in figure 9, left panel, we show MORGANA cooling flow versus star formation for all the central galaxies present in the box at  $z = 2.5$ . The stronger starbursts are associated with the stronger cooling flows<sup>3</sup>. Second, we show for the same halos (right panel) the

ratio of classical and MORGANA cooling flows versus star formation. For massive starbursts ( $\dot{M}_{\text{sf}} > 100 M_{\odot} \text{ yr}^{-1}$ ) the classical model predicts cooling flows a factor of 5-10 lower, which would presumably result in correspondingly lower star formation rates. The relation changes at smaller star formation rates, where feedback has been able to suppress the MORGANA cooling flow in many cases<sup>4</sup>. The success of MORGANA should then be ascribed to the different modeling of cooling.

With our model we can also investigate the physical conditions of SCUBA sources. In fig. 10a we show the star-formation function of galaxies at  $z = 2.5$ , divided into bulges (mergers) and discs. In this case, we use the punctual value of the star formation rate computed at the end of the time bin. Interestingly, mergers dominate only at the highest star formation rates,  $\gtrsim 200 M_{\odot} \text{ yr}^{-1}$ . This implies that most of our starbursts are triggered by cooling/infall more than by mergers, in line with the findings of violently star-forming discs at  $z \sim 2$  (Genzel et al. 2006). However, this does not imply that massive starbursts are associated with spiral galaxies. In Fig. 10b the star formation rate is computed as the total amount of stars formed in the 0.1 Gyr time bin and eventually found (at the end of the time bin) in a bulge or disc component, divided by the width of the time bin. This time bulges clearly dominate the star-formation function. This shows that such massively star-forming discs

already quenched cooling, or where cooling has already deposited most mass in the galaxy

<sup>4</sup> Many points at low star-formation lie out of this plot because the classical model predicts no cooling, while in MORGANA gas is still present due to feedback and cosmological infall.

<sup>3</sup> A few massive starburst are associated with no cooling flow and then lie outside this relation; these are mergers where feedback has

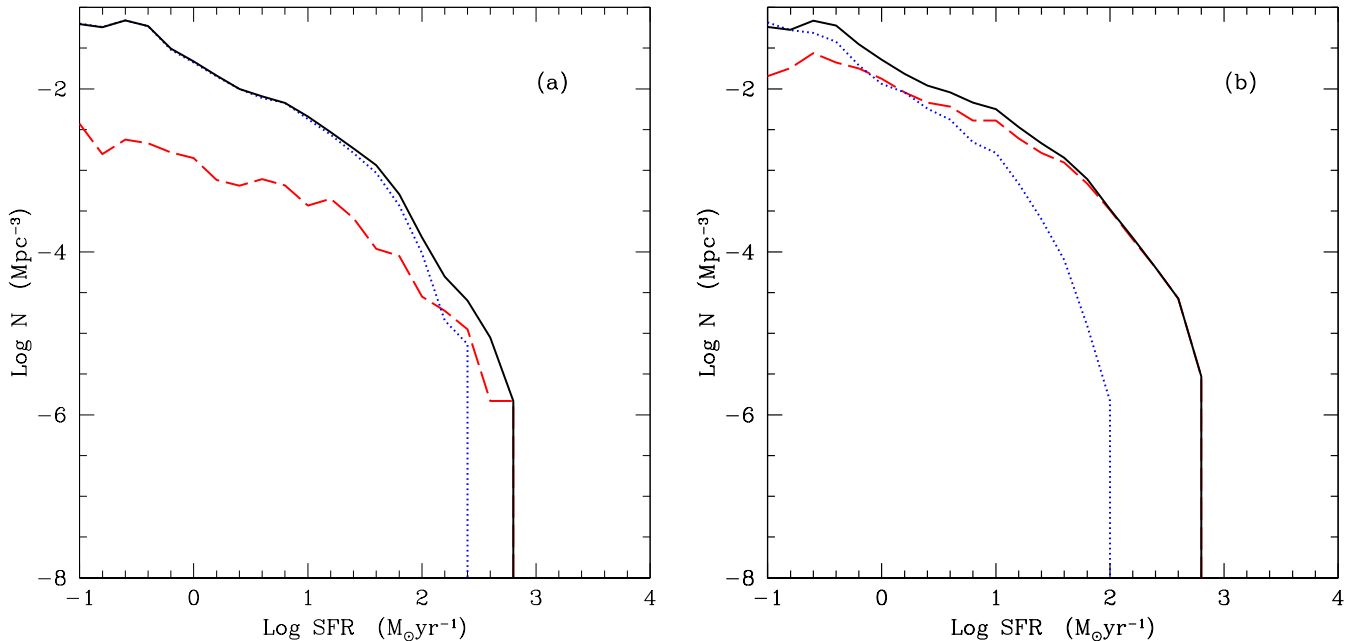


**Figure 10.** Star-formation rate function at  $z = 2.5$  for discs (blue dotted line), bulges/mergers (red dashed line) and total (black continuous line). The star formation in panel (a) is the punctual value at the end of the integration over the time bin, in (b) is the average in the bin (of width 0.1 Gyr) relative to the stars contained in bulges and discs at the end of the integration.

merge into bulges (disc instabilities are not relevant at this redshift) in less than 0.1 Gyr. Such short time-scales guarantee high levels of  $\alpha$ -enhancement, so the stellar populations formed in these starbursts will be typical of early-type galaxies. We conclude that the cooling/infall domination of high-redshift starbursts does not change the conclusion that these events are responsible for the formation of the stars found today in elliptical galaxies.

The overall agreement between model and data is in line with recent results by De Lucia et al. (2006), Bower et al. (2006), Croton et al. (2006) and Kitschichler & White (2006). However, there are three main points of disagreement between our model and the data. First, the evolution of the most massive galaxies at  $z < 1$  is too strong, resulting in an excess of bright galaxies in the K-band. It is easy to absorb this excess at  $z = 0$  by tuning the parameters, but this would be done at the expense of a poor fit of the stellar mass function and K-band LF at  $z \sim 1$ . As demonstrated by Monaco et al. (2006), this evolution is driven by galaxy mergers, so no feedback recipe can solve it. Our implementation of the suggestion of Monaco et al. (2006) to scatter 40% stars to the diffuse component of galaxy clusters at each merger goes in the right direction but is largely insufficient to suppress this evolution. A much higher scattered fraction, like  $\sim 80\%$  of the stellar mass of the satellite, would give a better results (as argued also by Conroy et al. 2007 and Renzini 2007). However, such an extreme value applied to all mergers and all redshift does not allow to reproduce the  $\sim 1\%$  fraction of diffuse stars in the Milky Way together with the  $\sim 10\%$  fraction in Virgo and the  $\sim 40\%$  fraction in massive clusters. We conclude that, while the mechanism is promising and deserves further attention, an easy and straightforward implementation does not work; this mecha-

nism should be selectively efficient in the most massive DM halos at low redshift.

Second, the model is not able to reproduce the most luminous SCUBA galaxies at redshift  $z \sim 2$ , which correspond to the strongest starbursts. This also hints to an insufficient “downsizing” in our predicted galaxy population. In the most massive galaxies the fraction formed at high redshift in episode of intense star formation is still too small, and the fraction of stars accreted at later times is still too large, with respect to the observed trends. Given the success in reproducing the bulk of the SCUBA population, a detailed investigation on the predictions of the cooling/infall model in the more massive halos is promising. Also the choice of a less conservative IMF, i.e. the Kroupa IMF, can help to solve the problem, thanks to the larger number of massive stars predicted at each stellar generation.

Third, we confirm the finding of Fontana et al. (2006) that our model produces too many faint objects at  $z \sim 1$ ; in other words, our smaller galaxies are too old. Coupled with the excessive evolution of the most massive galaxies, this finding shows that, while reproducing the average build-up of galaxies, the observed trend of less massive galaxies being on average younger is not properly reproduced by MORGANA. Fontana et al. (2006) have shown very convincingly that this problem is shared by many galaxy formation codes, either numerical or semi-analytic, so our results can be considered as the typical outcome of the  $\Lambda$ CDM cosmogony, given the present understanding of the physics of galaxy formation. Figure 11 shows a comparison of the evolution of the stellar mass function as inferred by the GOODS-MUSIC sample and as predicted by MORGANA. Clearly, the “downsizing” trend of more massive galaxies evolving very slowly at  $z < 1$ , while the population of less massive galaxies builds up, is

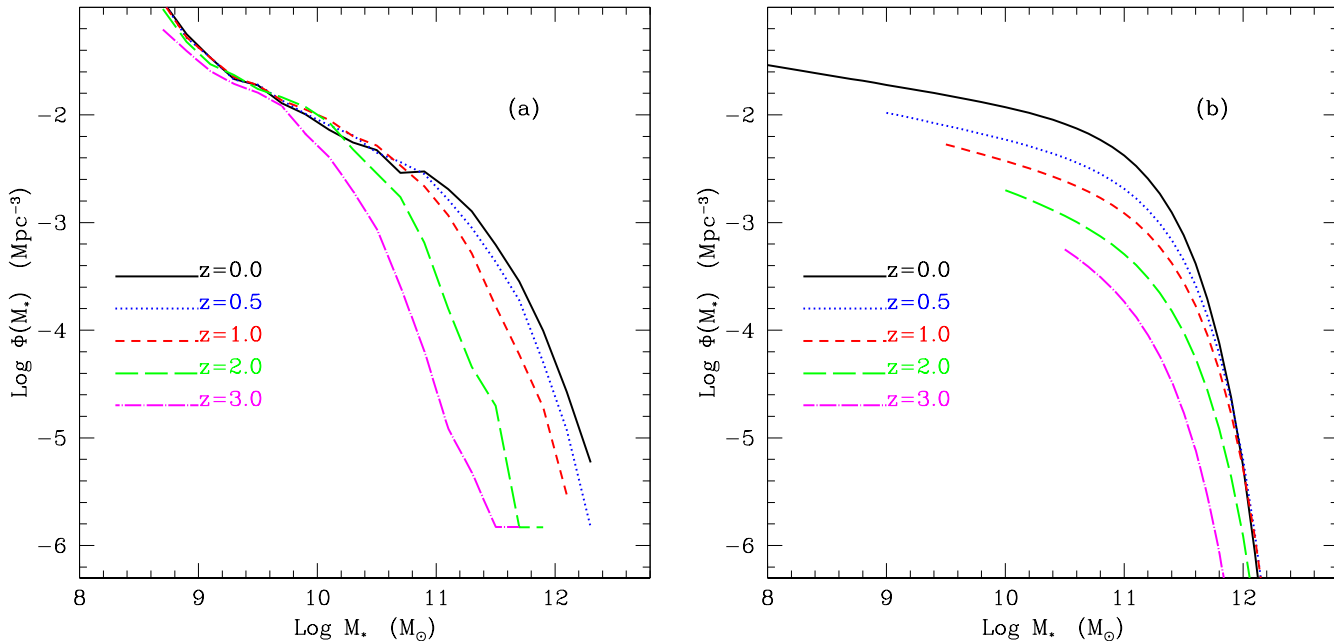


**Figure 11.** Evolution of the stellar mass function according to MORGANA (panel a) and GOODS-MUSIC (panel b). The latter mass functions are drawn roughly in the same mass interval where data are available.

not reproduced. While the evolution of the high-mass end is driven by mergers, a delay in the build-up of faint galaxies should be caused by some source of feedback.

## 5 CONCLUSIONS

This paper is the third of a series devoted to presenting MORGANA. We have demonstrated that the model is able to follow the build-up of the bulk of stars, more precisely to reproduce the early assembly and late, almost-passive evolution of massive galaxies. To this aim we have combined MORGANA with GRASIL and compared predictions with observation in the submm (the  $850\mu\text{m}$  channel), especially sensitive to the strongest and most obscured episodes of star formation, and in the NIR (especially in the  $K$ -band), most sensitive to the stellar mass. Overall consistency between model and observations has been obtained using SCUBA counts at  $850\mu\text{m}$ , number counts in the  $K$ -band, redshift distribution of  $K$ -limited galaxy samples, and redshift evolution of the  $K$ -band LF. The importance of this result is strengthened by the use of a standard Salpeter IMF (e.g. a very conservative choice) along the whole redshift interval. We ascribe this agreement mostly to our improved model for cooling/infall, that correctly reproduces the results controlled numerical experiments.

We predict that most star formation at high redshift is not stimulated by starbursts but is due to the strong cooling/infall flows that take place at early times. This does not imply that such discs are close analogues of local spiral galaxies, as their gas surface density is very high, their star formation rate is typical of starburst galaxies and most of them are expected to merge within less than 0.1 Gyr. We then predict that gas-rich discs, characterized by star-

formation rates up to  $100 - 200 M_{\odot} \text{ yr}^{-1}$ , should be very abundant at  $z \sim 2$ , in line with the observations of Genzel et al. (2006).

Despite these successes, our model does not reproduce the “downsizing” trend of a modest evolution of the most massive galaxies accompanied by a build-up of small galaxies at  $z \lesssim 1$ . We propose that a solution of this discrepancy requires at least two mechanisms, because the evolution of the bright end is driven by inevitable galaxy mergers, while star formation in less massive galaxies is sensitive to feedback. The solution proposed by Monaco et al. (2006) for slowing the evolution of massive galaxies requires an implementation of scattering of stars to the diffuse component that is strongly dependent on DM halo mass and/or redshift. On the other hand, a solution of the overabundance of  $10^{11} M_{\odot}$  galaxies at  $z \sim 1$ , common to most galaxy formation models (Fontana et al. 2006), calls for some unknown source of feedback.

## ACKNOWLEDGMENTS

We thank Stefano Cristiani, Andrea Cimatti, Gianluigi Granato, Adriano Fontana, Alvio Renzini, Carlos Frenk, Cedric Lacey, Rachel Somerville and Eric Bell for many enlightening discussions; we also thank Lucia Pozzetti for providing the VVDS redshift distribution. PM thanks the ICC of Durham for its hospitality. Calculations were carried out both at the “Centro Interuniversitario del Nord-Est per il Calcolo Elettronico” (CINECA, Bologna) with CPU time assigned under University of Trieste/CINECA grants, and at the PIA cluster of the Max-Planck-Institut für Astronomie at the Rechenzentrum Garching.

REFERENCES

Aretxaga, I., Hughes, D.H., Coppin, K., et al., 2007, MNRAS, 379, 1571

Barger, A. J., Cowie, L. L., Sanders, D. B., 1999, ApJL, 518, L5

Baugh C.M., Lacey C.G., Frenk C.S., Granato G.L., Silva L., Bressan A., Benson A.J., Cole S., 2005, MNRAS, 356, 1191

Benson, A. J., Bower, R. G., Frenk, C. S., Lacey, C. G., Baugh, C. M., & Cole, S. 2003, ApJ, 599, 38

Bernardi, M., et al. 2003, AJ, 125, 1866

Blakeslee, J. P., et al. 2003, ApJL, 596, L143

Borys, C., Chapman, S. C., Halpern, M., Scott, D., 2003, MNRAS, 344, 385

Borys, C., Chapman, S. C., Halpern, M., Scott, D., 2002, MNRAS, 330, L63

Bower R. G., Benson A. J., Malbon R., Helly J. C., Frenk C. S., Baugh C. M., Cole S., Lacey C. G. 2006, MNRAS, 370, 645

Bressan, A., Granato, G. L., Silva, L., 1998, A&A, 332, 135

Bressan, A., Silva, L., Granato, G.L., 2002, A&A, 392, 377

Cattaneo A., Dekel A., Devriendt J., Guiderdoni B., Blaizot J., 2006, MNRAS, 370, 1651

Cimatti, A., et al. 2004, Nat, 430, 184

Cimatti, A., et al. 2002b, A&A, 391, 1

Cimatti, A., Daddi, E., & Renzini, A. 2006, A&A, 453, L29

Cirasuolo, M., et al., 2007, MNRAS, 380, 585

Chapman, S. C., Scott, D., Borys, C., Fahlman, G. G., 2002, MNRAS, 330, 92

Chapman, S.C., Blain, A.W., Ivison, R.J., Smail, I.R., 2003, Nat., 422, 695

Chapman, S.C., Blain, A.W., Smail, I.R., Ivison, R.J., 2005, ApJ, 622, 772

Cole, S., Lacey, C.G., Baugh, C.M., & Frenck, C.S., 2000, MNRAS, 319, 168

Cole, S., Norberg, P., Baugh, C.M., et al., 2001, MNRAS, 326, 255

Conroy, C., Weschler, R.H., & Kravtsov A.V., 2007, (astro-ph/0703374)

Coppin, K., Chapin, E.L., Mortier, A.M.J., et al., 2006, MNRAS, 372, 1621

Cowie, L. L., Barger, A. J., Kneib, J.-P., 2002, AJ, 123, 2197

Croton, D.J. et al., 2006, MNRAS, 365, 11

Daddi, E., et al. 2002, A&A, 384, L1

Davis, M., et al. 2003, Proc. SPIE, 4834, 161

De Lucia G., Springel V., White S. D. M., Croton D., Kauffmann G., 2006, MNRAS, 366, 499

De Lucia, G., & Blaizot, J. 2007, MNRAS, 375, 2

Devriendt, J. E. G., & Guiderdoni, B., 2000, A&A, 363, 851

Djorgovski, S., et al. 1995, ApJ, 438, L13

Dye, S., et al. 2006, MNRAS, 372, 1227

Eales, S., Lilly, S., Webb, T., Dunne, L., Gear, W., Clements, D., Yun, M., 2000, AJ, 120, 2244

Eke V. R., Navarro J. F., Steinmetz M., 2001, ApJ, 554, 114

Ellis, S. C., Jones, L. R., Donovan, D., Ebeling, H., & Khosroshahi, H. G. 2006, MNRAS, 368, 769

Fontana A., et al., 2006, A&A, 459, 745

Fontanot F., Monaco P., Cristiani S., Tozzi P., 2006 MNRAS, 373, 1173

Firth, A.E., Somerville, R.S., McMahon, R.G., et al., 2001

Gardner, J.P., Cowie, L.L., Wainscoat, R.J., 1993, ApJ 415, 9

Gardner, J.P., Sharples, R.M., Carrasco, B.E., Frenk, C.S., 1996, MNRAS, 282, 1

Gavazzi, G., Pierini, D. & Boselli, A., 1996, A&A, 312, 397

Giavalisco, M., Ferguson, H. C., Koekemoer, A. M., et al. 2004, ApJ, 600, L93

Glazebrook, K., Peacock, J.A., Collins, C.A., Miller, L. 1994, MNRAS, 266, 65

Granato, G. L., Lacey, C. G., Silva, L., Bressan, A., Baugh, C. M., Cole, S., Frenk, C. S., 2000, ApJ, 542, 710

Granato G.L., De Zotti G., Silva L., Bressan A., Danese L., 2004, ApJ, 600, 580

Grazian, A., et al. 2006, A&A, 449, 951

Guiderdoni, B., Hivon, E., Bouchet, F. R., Maffei, B., 1998, MNRAS, 295, 877

Hughes, D. H., et al. 1998, Nat, 394, 241

Iovino, A., et al. 2005, A&A, 442, 423

Le Fevre, O., Vettolani, G., Garilli, B., et al., 2005, A&A, 439, 845

Kang X., Jing Y. P., Mo H. J., Börner G., 2005, ApJ, 631 21

Keres D., Katz N., Weinberg D. H., Davé R., 2005, MNRAS, 363, 2

Kennicutt, R.C., 1989, ApJ, 344, 685

Kochanek, C.S., Pahre, M.A., Falco, E.E. et al. 2001, ApJ, 560, 566

Kodama, T., Arimoto, N., Barger, A. J., & Aragón-Salamanca, A. 1998, A&A, 334, 99

Kong, X., et al. 2006, ApJ, 638, 72

Lawrence, A., et al. 2007, MNRAS, 379, 1599

Maihara, T., et al. 2001, PASJ, 53, 25

Maraston, C., 2005, MNRAS, 362, 799

Matteucci, F. 1996, ASP Conf. Ser. 98: *From Stars to Galaxies: the Impact of Stellar Physics on Galaxy Evolution*, 98, 529

Menci N., Cavaliere A., Fontana A., Giallongo E., Poli F., Vittorini V., 2004, ApJ, 604, 12

Mo, H.J., Mao, S., White, S.D.M., 1998, MNRAS, 295, 319

Mo, H. J., Mao, S., 2000, MNRAS, 318, 163

Mobasher, B., Ellis, R.S., Sharples, R.M., 1996, MNRAS, 223, 11

Moustakas, L.A., Davis, M., Graham, J.R., Silk, J., Peterson, B.A., Yoshii, Y. 1997, ApJ, 475, 445

Monaco P., Theuns T., Taffoni G., 2002, MNRAS, 331, 587

Monaco, P., 2004, MNRAS, 352, 181

Monaco, P., 2004b, MNRAS, 354, 151

Monaco, P., & Fontanot, F. 2005, MNRAS, 359, 283

Monaco, P., Murante, G., Borgani, S., Fontanot, F., 2006, ApJL, 652, 89

Monaco, P., Fontanot, F. & Taffoni, G., 2007, MNRAS, 375, 1189

Murante, G., Giovalli, M., Gerhard, O., Arnaboldi, M., Borgani, S., & Dolag, K. 2007, MNRAS, 377, 2

Nagashima M., Lacey C. G., Okamoto T., Baugh C. M., Frenk C. S., Cole S., 2005, MNRAS, 363, L31

Nagamine, K., Cen, R., Hernquist, L., Ostriker, J. P., Springel, V. 2005a, ApJ, 618, 23

Neisteinn E., van den Bosch F. & Dekel A., 2006, MNRAS 372 933

- Panuzzo, P., Bressan, A., Granato, G. L., Silva, L., Danese, L., 2003, *A&A*, 409, 99
- Pozzetti, L., Cimatti, A., Zamorani, G. et al., 2003, *A&A*, 402, 837
- Pozzetti, L., et al., 2007, (astro-ph/0704.1600)
- Refregier A., 2003, *ARA&A*, 41, 645
- Renzini, A., & Ciotti, L. 1993, *ApJL*, 416, L49
- Rix, H.-W., Bardeen, M., Beckwith, S.V.W., et al., 2004, *ApJS*, 152, 163
- Robertson et al. 2007 (astro-ph/0703456)
- Saro, A., Borgani, S., Tornatore, L., Dolag, K., Murante, G., Biviano, A., Calura, F., & Charlot, S. 2006, *MNRAS*, 373, 397
- Scoville, N., et al. 2007, *ApJS*, 172, 1
- Scott, S. E., Fox, M. J., Dunlop, J. S., Serjeant, S., et al., 2002, *MNRAS*, 331, 817
- Silva, L., 1999, PhD Thesis
- Silva, L., Granato, G.L., Bressan, A., Danese, L., 1998, *ApJ*, 509, 103
- Silva, L., De Zotti, G., Granato, G. L., Maiolino, R., & Danese, L. 2005, *MNRAS*, 357, 1295
- Smail, I., Ivison, R., Blain, A., 1997, *ApJ*, 490, L5
- Smail, I., Ivison, R., Blain, A., Kneib, J.-P., 2002, *MNRAS*, 331, 495
- Smith, G.P., Smail, I., Kneib, J.P., et al., 2001
- Somerville, R. S., Primack, J. R., & Faber, S. M. 2001, *MNRAS*, 320, 504
- Somerville, R. S., Moustakas, L.A., Mobasher, B., et al., 2004, *ApJ*, 600, 135
- Spergel, D.N., et al., 2007, *ApJS*, 170, 377
- Springel V. et al., 2005, *Nat*, 435, 629
- Szokoly, G.P., Subbarao, M.U., Connolly, A.J., Mobasher, B., 1998, *ApJ*, 492, 452
- Sutherland R. & Dopita M., 1993, *ApJS*, 88, 253
- Taffoni, G., Mayer, L., Colpi, M., Governato, F., 2003, *MNRAS*, 341, 434
- Taffoni, G., Monaco, P., Theuns T., 2002, *MNRAS*, 333, 623
- Thomas, D., Maraston, C., Bender, R., & de Oliveira, C. M. 2005, *ApJ*, 621, 673
- Umemura M., 2001, *ApJ*, 560, L29
- Volonteri, M., Haardt, F., & Madau, P. 2003, *ApJ*, 582, 559
- Vega, O., Silva, L., Panuzzo, P., Bressan, A., Granato, G. L., Chavez, M., 2005, *MNRAS*, 364, 1286
- Viola, M., Borgani, S., Monaco, P., Murante, G., Tornatore, L., 2007, *MNRAS*, to be submitted
- Webb, T., Eales, S., Lilly, S., Clements, D., Dunne, L., Gear, W., Flores, H., Yun, M., 2003, *ApJ*, 587, 41
- White, S. D. M. 1996, *Cosmology and Large Scale Structure*, 349
- Wolf, C., Meisenheimer, K., Röser, H.-J. 2001, *A&A*, 365, 660
- Wu, K.K.S., Fabian, A.C., Nulsen, P.E.J., 2001, *MNRAS*, 318, 889
- Zheng, X. Z., Bell, E. F., Papovich, C., Wolf, C., Meisenheimer, K., Rix, H.-W., Rieke, G. H., & Somerville, R. 2007, *ApJL*, 661, L41